Multicarrier Relay Selection for Full-Duplex Relay-Assisted OFDM D2D Systems

Shuping Dang, *Student Member, IEEE*, Gaojie Chen, *Member, IEEE* and Justin P. Coon, *Senior Member, IEEE*

***Abstract*—In this paper, we propose a full-duplex orthogonal frequency-division multiplexing (OFDM) device-to-device (D2D) system in two-hop networks, where multiple full-duplex decode-and-forward (DF) relays assist the transmission from D2D user equipment (DUE) transmitter to DUE receiver. By such a transmission mechanism, the signal transmitted by the DUE transmitter does not need to go through a base station (BS). Meanwhile, due to the adoption of underlay D2D communication protocol, power control mechanisms are thereby necessary to be applied to mitigate the interference to conventional cellular communications. Based on these considerations, we analyze the outage performance of the proposed system, and derive the exact expressions of outage probabilities when bulk and per-subcarrier relay selection criteria are applied. Furthermore, closed-form expressions of outage probabilities are also obtained for special cases when the instantaneous channel state information (CSI) between BS and cellular user equipments (CUEs) is not accessible, so that a static power control mechanism is applied. Subsequently, we also investigate the outage performance optimization problem by coordinating transmit power among DUE transmitter and relays, and provide a suboptimal solution, which is capable of improving the outage performance. All analyses are substantiated by numerical results provided by Monte Carlo simulations. The analytical and numerical results demonstrated in this paper can provide an insight into the full-duplex relay-assisted OFDM D2D systems, and serve as a guideline for its implementation in next generation networks.**

***Index Terms*—Device-to-device (D2D) communications, multicarrier relay selection, full-duplex system, OFDM, outage performance.**

I. Introduction

With a rapidly increasing demand of communication services in recent years, existing communication technologies relying on infrastructure, e.g. access point (AP) and base station (BS), will soon be insufficient to meet the requirements of ubiquitous communications in the near future [1]. As a result, device-to-device (D2D) communication has attracted a considerable amount of attention in recent years and been regarded as a promising technology for next generation networks due to its high power efficiency, high spectral efficiency and low transmission delay [2]–[4]. D2D communication enables the direct wireless transmission between two devices (a.k.a. D2D user equipments (DUEs)) in proximity, without going through a BS. Such a flexible transmission protocol releases the design requirements of infrastructure and thereby saves transmission overheads caused by centralized coordination and management [2]. Meanwhile, D2D communications can be classified in two categories, depending on whether frequency resources are shared between D2D communications and traditional cellular communications, which are termed *underlay* and *overlay* D2D communications, respectively [2]. It has been proved that underlay D2D communications would be able to provide a high spectrum efficiency and suit the spectrum sharing nature in next generation networks [5]–[7]. However, the underlay D2D transmission will break up the orthogonality between D2D communications and traditional cellular communications, and the corresponding interference shall be coordinated accordingly.

On the other hand, conventional D2D communications requiring a strong direct link between DUEs might not always be feasible in practice, as the direct link could be in deep fading and shadowing due to the existence of physical obstacles. In this scenario, D2D communications will become impractical or require a huge amount of transmit power, which will result in severe interference to cellular communications and significantly degrade the overall system performance [8]. To solve this problem and enhance the applicability of D2D communications, relay-assisted D2D communication was proposed with decode-and-forward (DF) relays and amplify-and-forward (AF) relays in [9] and [8], respectively. However, there is no exact analytical results provided in these two pioneering works. Then, the power control strategy and energy-related issues for relay-assisted D2D communications were numerically studied in [10] and [11]. Moreover, some practical aspects of relay-assisted D2D communication systems, e.g. transmission capacity and delay performance were investigated in [12] and [13].

To further enhance the performance of relay-assisted D2D systems, recent research also focuses on the employment of full-duplex relays, as it would double the transmission rate, as long as the self-interference (SI) can be dealt with appropriately [14]–[16]. In [14], the authors proposed a novel underlay D2D communication scheme, which dynamically assigns DUE transmitters as full-duplex relays to assist cellular downlink transmissions. In [15], the coverage probability is analyzed for the D2D communication scenario, in which cellular user equipments (CUEs) are assisted by full-duplex relays. A simple case of a pair of DUEs assisted by only one full-duplex relay is discussed in [16]. However, the aforementioned works have not considered the application of multicarrier paradigms, which degrades their practicability in next generation networks [17]. At the time of writing, the only two works incorporating D2D systems and multicarrier paradigms are given in [18], [19]. However, these works only employ optimization techniques to provide numerical results without giving much insight into the multicarrier D2D system *per se*.

Therefore, to fill the gap between relay-assisted D2D communi-

This work was supported by the SEN grant (EPSRC grant number EP/N002350/1) and the grant from China Scholarship Council (No. 201508060323).

S. Dang and J.P. Coon are with the Department of Engineering Science, University of Oxford, Oxford, U.K., OX1 3PJ (e-mail: {shuping.dang, justin.coon}@eng.ox.ac.uk).

G. Chen is with the Department of Engineering, University of Leicester, Leicester, U.K., LE1 7RH (email: gaojie.chen@leicester.ac.uk).

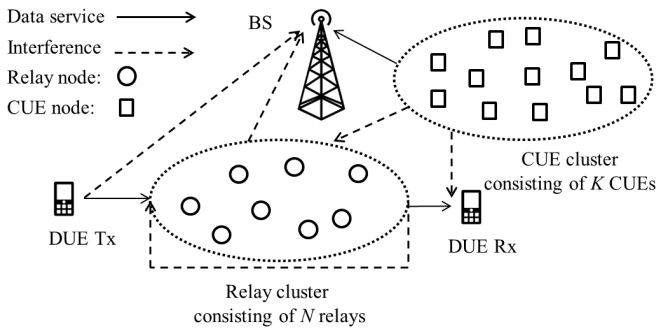

Fig. 1: Network model for the proposed full-duplex relay-assisted D2D system, containing one BS, K CUEs in a CUE cluster, N relays in a relay cluster, one DUE transmitter (source) and one DUE receiver (destination).

cations and multicarrier paradigms and provide a comprehensive analysis, we propose a full-duplex orthogonal frequency-division multiplexing (OFDM) D2D system assisted by multiple relays and analyze its outage performance in this paper. To be specific, the DF forwarding protocol with bulk and per-subcarrier relay selections is taken into consideration, which makes the proposed system more realistic for practical scenarios. To summarize, the contributions of this paper are listed infra:

1) We propose a more practical system model combining relay-assisted D2D communications, OFDM systems, full-duplex transmissions and multicarrier relay selections, which suits the nature of next generation networks.
2) We analyze the outage performance of the proposed system with multiple DF relays applying two different relay selection schemes.
3) We derive the exact expressions of outage probabilities for all scenarios as well as the closed-form expressions for some special cases and numerically verify them. Also, by two ideal conditions, the outage floors for the static power control mechanism can be derived in neat and closed forms, which clearly reveal the relations among outage performance and system parameters.
4) We formulate an optimization problem for the outage performance and propose suboptimal solutions to efficiently yield a better outage performance.

The rest of this paper is organized as follows. We present the system model in Section II. Then, outage performance for different relay selection schemes is analyzed in Section III. After that, we formulate the outage performance optimization problem and provide suboptimal solutions in Section IV. Subsequently, all analyses are numerically verified by Monte Carlo simulations in Section V. Finally, the paper is concluded in Section VI. As there are many notations used in this paper, for readers' convenience, we list the key notations in Table I.

TABLE I: Key notations used in this paper

Notation	Definition/explanation
α	Preset power coordination factor
α^*	Optimal power coordination factor
$\alpha^{\&}$	Suboptimal power coordination factor
$E_n(x)$	$E_n(x)=\int_1^\infty e^{-xt}/t^n \mathrm{d}t$ denotes the exponential integral function
$\mathscr{E}_n(x)$	$\mathscr{E}_n(x)=xe^xE_n(x)$ is a defined function
$G_{ij}(k)$	Instantaneous channel power gain between node i and node j over the kth subcarrier
μ_{ij}	Average channel power gain between node i and node j
$\Gamma(a,x)$	$\Gamma(a,x)=\int_x^\infty t^{a-1}e^{-t}\mathrm{d}t$ denotes the incomplete gamma function
κ	Static power control factor
K	Number of subcarriers/CUEs
$\mathcal{K}$	Set of subcarriers
N	Number of relays
$\mathcal{N}_R$	Set of relays
$\mathcal{N}_C$	Set of CUEs
$\mathcal{N}_{bulk}$	Set of relay selected by bulk relay selection
$\mathcal{N}_{ps}$	Set of relays selected by per-subcarrier relay selection
$\tilde{n}(k)$	Index of the selected relay forwarding the kth subcarrier
P_C	CUE transmit power
$\bar{P}_S$	Maximum allowed transmit power at the DUE transmitter
$\bar{P}_R$	Maximum allowed transmit power at relays
$P_S(k)$	Instantaneous transmit power on the kth subcarrier at the DUE transmitter
$P_{R_n}(k)$	Instantaneous transmit power on the kth subcarrier at the nth relay
s	Preset outage threshold for D2D communications
ξ	Preset outage threshold for cellular communications
$\varphi_n(k)$	Instantaneous power of the residual SI at the nth relay for the kth subcarrier
$\bar{\varphi}$	Average power of the residual SI

II. System Model

A. System Framework

The framework of the proposed system is presented in Fig. 1, where one BS, a pair of DUE transmitter and receiver, a cluster of N full-duplex DF relays and a cluster of K cellular user equipments (CUEs) are considered. Their shorthand notations are B, S, D, R_n and C_k, respectively, $\forall\, n \in \mathcal{N}_R = \{1,2,\ldots,N\}$ and $\forall\, k \in \mathcal{N}_C = \{1,2,\ldots,K\}$. Meanwhile, by employing OFDM, it is supposed that there exist K independent subcarriers allocated to K CUEs and used by CUEs and DUEs in an underlay manner. The set of these K subcarriers is denoted as $\mathcal{K} = \{1,2,\ldots,K\}$. In other words, there is a unique bijective mapping relation between $\mathcal{N}_C$ and $\mathcal{K}$, in order to mitigate the interference among CUEs and optimize the multiplexing gain of the cellular network[1].

From Fig. 1, it is obvious that the signal and interference transmissions are in an uplink scenario[2]. Therefore, the existing interference can be classified into three categories: 1) interference from active CUEs to DUE receiver and selected relay(s); 2)

[1]Here, we omit the subcarrier allocation process for CUEs, and assume it to be a *fait accompli* as a system configuration in this paper. Details of OFDM subcarrier allocation for multiuser scenarios can be found at [20]–[22].

[2]Most D2D communication systems are designed to utilize uplink cellular resources, because D2D users can monitor the received power of downlink control signals to estimate the channel between the DUE transmitter and the BS [2]. Therefore, this will help maintain the transmit power of the DUE transmitter below a threshold, so that the interference caused by D2D communications to cellular systems can be mitigated effectively [23]. Another reason to use the uplink resource for D2D transmission is to avoid the severe interference caused by the transmission from BS, as BS normally transmits by a much larger power than CUEs'. Following this common design guideline, we also assume that D2D communication utilizes uplink spectrum resources and the downlink scenario is out of the scope of this paper.

interference from DUE transmitter and selected relay(s) to BS; 3) SI at selected relay(s) because of the adoption of the full-duplex transmission protocol. According to the basic design guidelines of D2D communication networks [2], the cellular communications should be ensured with transmission priority, and the first interference is thereby inevitable in the proposed system. In order to deal with the second interference, we have to make sure that for the kth subcarrier, the received aggregate interference from DUE transmitter and selected relay(s) is mitigated below a certain level. Therefore, considering an interference-limited environment [24], a dynamic power control mechanism is applied at the DUE transmitter and selected relay(s) on the kth subcarrier, which can be written as:

$$P_S(k) = \min\left\{\frac{\alpha P_C G_{CB}(k)}{\xi G_{SB}(k)}, \bar{P}_S\right\} \tag{1}$$

and

$$P_{R_n}(k) = \min\left\{\frac{(1-\alpha) P_C G_{CB}(k)}{\xi G_{R_n B}(k)}, \bar{P}_R\right\}, \tag{2}$$

where P_C is the CUE transmit power and assumed to be the same for all CUEs; $\alpha \in (0,1)$ is a preset power coordination factor, which is used to coordinate the transmit power of DUE transmitter and relays and is the same among all subcarriers and relays; ξ is a preset outage threshold for cellular communications; $\bar{P}_S$ and $\bar{P}_R$ are the maximum allowed transmit power corresponding to DUE transmitter and relays on each subcarrier; $G_{ij}(k)$ denotes the channel power gain for the kth subcarrier, given $i \neq j$ and $i, j \in \{B, S, D\} \bigcup \mathcal{N}_R \bigcup \mathcal{N}_C$[3], and obeys the exponential distribution with the probability density function (PDF) and cumulative distribution function (CDF) given by

$$f_{G_{ij}}(g) = e^{-g/\mu_{ij}}/\mu_{ij} \quad \Leftrightarrow \quad F_{G_{ij}}(g) = 1 - e^{-g/\mu_{ij}}, \tag{3}$$

where μ_{ij} is the average channel power gain[4].

B. Decode-and-Forward Forwarding Protocol

Because of the interference-limited environment, we can neglect the effects of additive noise at receivers and express the instantaneous signal-to-interference ratio (SIR) from DUE transmitter to the nth relay (i.e. the first hop) on the kth subcarrier by

$$\Gamma_{SR_n}(k) = \frac{G_{SR_n}(k) P_S(k)}{P_C G_{CR_n}(k) + \varphi_n(k)}, \tag{4}$$

where $\varphi_n(k)$ denotes the power of residual SI at the nth relay for the kth subcarrier, and we assume that $\varphi_n(k)$ obeys the exponential distribution with PDF and CDF written as[5]

$$f_\varphi(g) = e^{-g/\bar{\varphi}}/\bar{\varphi} \quad \Leftrightarrow \quad F_\varphi(g) = 1 - e^{-g/\bar{\varphi}}, \tag{5}$$

where $\bar{\varphi}$ is the average power of residual SI.

Further assuming that there does not exist a direct transmission link between DUE transmitter and receiver due to deep fading[6], and the DF forwarding protocol is applied at all relays, we can express the SIR from the nth relay to the DUE receiver (i.e. the second hop) by

$$\Gamma_{R_n D}(k) = \frac{G_{R_n D}(k) P_{R_n}(k)}{P_C G_{CD}(k)}. \tag{6}$$

Subsequently, we can express the equivalent end-to-end instantaneous SIR for full-duplex DF relay-assisted systems by [29]

$$\Gamma_{SR_n D}(k) = \min\left\{\Gamma_{SR_n}(k), \Gamma_{R_n D}(k)\right\}. \tag{7}$$

C. Relay Selection Schemes

1) Bulk selection: In this paper, we adopt the instantaneous SIR as the performance metric to perform relay selections. By bulk selection, there will be only *one* relay selected out of N relays. The selection criterion can be written as

$$\mathcal{N}_{bulk} = \{\tilde{n}\} = \bigcup_{k\in\mathcal{K}} \{\tilde{n}(k)\} = \arg\max_{n\in\mathcal{N}_R} \min_{k\in\mathcal{K}} \{\Gamma_{SR_n D}(k)\}, \tag{8}$$

where $\tilde{n} = \tilde{n}(1) = \tilde{n}(2) = \cdots = \tilde{n}(K)$ is the index of the selected relay forwarding all K subcarriers, and $\tilde{n}(k)$ represents the index of the selected relay forwarding the kth subcarrier, $\forall\ k \in \mathcal{K}$. Bulk relay selection is easy to implement and will not involve a complicated coordination and synchronization among multiple relays. However, the performance resulted by bulk relay selection is far from optimal [30].

2) Per-subcarrier selection: On the other hand, by per-subcarrier selection, relays are selected by each individual subcarrier in a per-subcarrier manner and the set of all selected relays can be determined by

$$\mathcal{N}_{ps} = \bigcup_{k\in\mathcal{K}} \{\tilde{n}(k)\} = \bigcup_{k\in\mathcal{K}} \left\{\arg\max_{n\in\mathcal{N}_R} \{\Gamma_{SR_n D}(k)\}\right\}. \tag{9}$$

In contrast to bulk relay selection, per-subcarrier relay selection is optimal in terms of outage performance, while a much higher system complexity and signaling overhead are caused due to the coordination and synchronization among multiple relays [30]. Obviously, these bulk and per-subcarrier relay selection schemes can be regarded as two extremes in the performance-complexity trade-off of multicarrier relay selection and thus are representative. Therefore, this motivates us to introduce both schemes to relay-assisted OFDM D2D systems and carry out the analysis in this paper.

Meanwhile, both bulk and per-subcarrier relay selections can be carried out in practice by a timer-based distributed implementation scheme, which releases the requirement of centralized signaling and coordination and is thereby suited for D2D communications [31]. For clarity, a pictorial illustration of the bulk and per-subcarrier selections is presented in Fig. 2.

[3]In this paper, we assume that all channels are reciprocal and therefore have $G_{ij}(k) = G_{ji}(k)$.

[4]Because of relay and CUE clusters, we can further assume that the sizes of clusters are relatively small compared to the scale of the network. As a result, we can have the uniform μ_{SR}, μ_{RD}, μ_{CR}, μ_{CD}, μ_{RB}, μ_{CB} for all relays and CUEs [25]. Following this assumption, we can integrate all CUEs using K single subcarriers in the CUE cluster into a logically intact CUE, termed *integrated CUE*, which uses multiple subcarriers. Such an equivalent processing will ease the analysis in following sections.

[5]Admittedly, there are also works, in which Ricean distribution is employed to model the residual SI channel, since the channel can also be regarded as a line-of-sight (LOS) path [26]. However, according to further works on SI channel modeling [27], the adoption of SI channel model is subject to practical situations and employed interference cancellation techniques. Therefore, without loss of generality, we choose Rayleigh distribution in this paper to model the SI channel and thus the channel power gain is exponentially distributed. By varying the average channel power gain $\bar{\varphi}$, we can easily characterize the SI cancellation capability.

[6]Although D2D communications were raised for short-distance scenarios at the very beginning, with the help of relays, D2D communications currently become applicable to general scenarios considering moderate- and long-distance transmissions [28], which justifies the no-direct-transmission assumption here.

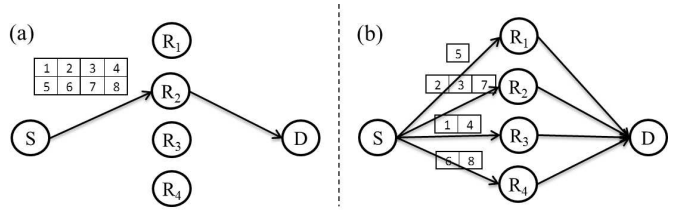

Fig. 2: Illustration of (a) bulk relay selection; (b) per-subcarrier relay selection.

D. Outage Probability

After relay selection, we can define the outage event of OFDM systems by [32]

Definition 1: An outage occurs when the end-to-end SIR of any subcarrier falls below a preset outage threshold s.

1) Full-duplex systems: The full-duplex transmission would potentially have an outage performance benefit, if the power of residual SI can be managed below a certain level by a series of SI cancellation technologies [33]. Consequently, we adopt the full-duplex transmission protocol in this paper for relay forwarding. As a result, for full-duplex systems, we can express the outage probability after relay selection as

$$P_{out}(s) = \mathbb{P}\left\{\min_{k\in\mathcal{K}}\left\{\Gamma_{SR_{\tilde{n}(k)}D}(k)\right\} < s\right\}, \tag{10}$$

where $\mathbb{P}\{\cdot\}$ denotes the probability of the event enclosed.

2) Half-duplex systems: As an important comparison benchmark of full-duplex systems, we also give the outage probability for half-duplex systems as follows [16]:

$$P_{out}^{half}(s) = \mathbb{P}\left\{\min_{k\in\mathcal{K}}\left\{\Gamma_{SR_{\tilde{n}(k)}D}^{half}(k)\right\} < s(s+2)\right\}, \tag{11}$$

where $\Gamma_{SR_{\tilde{n}(k)}D}^{half}(k) = \Gamma_{SR_{\tilde{n}(k)}D}(k)|_{\varphi_{\tilde{n}(k)}=0}$.

III. Outage Performance Analysis

By observing (1), (2) and (7), we can find that $G_{CB}(k)$ is a common term in the first and second hops and will result in a correlation between two hops. Moreover, $G_{CD}(k)$ and $G_{SB}(k)$ will lead to correlations among relays when performing relay selections. In order to carry out analysis without considering these correlation terms, we can temporarily let them be fixed values, say $G_{CB}(k) = \bar{g}(k)$, $G_{CD}(k) = \bar{h}(k)$ and $G_{SB}(k) = \bar{l}(k)$. As a consequence, the SIRs corresponding to different relays and subcarriers can be regarded as independent. Now we can define the conditional *a priori* outage probability, (i.e., the outage probability not conditioned on any form of relay selection having taken place) for the kth subcarrier forwarded by an arbitrary relay in the first and second hops as

$$\Xi_1\left(k|\bar{g}(k),\bar{l}(k)\right) = \mathbb{P}\left\{\Gamma_{SR_n}(k) < s|\bar{g}(k),\bar{l}(k)\right\}, \tag{12}$$

and

$$\Xi_2\left(k|\bar{g}(k),\bar{h}(k)\right) = \mathbb{P}\left\{\Gamma_{R_nD}(k) < s|\bar{g}(k),\bar{h}(k)\right\}. \tag{13}$$

Consequently, due to the bottleneck effect of two-hop DF relay networks (c.f. (7)), the conditional end-to-end *a priori* outage probability can be determined by

$$\begin{aligned}\Xi(k|\bar{g}(k),\bar{h}(k),\bar{l}(k)) = \Xi_1(k|\bar{g}(k),\bar{l}(k)) + \Xi_2(k|\bar{g}(k),\bar{h}(k))\\ - \Xi_1(k|\bar{g}(k),\bar{l}(k))\Xi_2(k|\bar{g}(k),\bar{h}(k)).\end{aligned} \tag{14}$$

To carry out further analysis, we should now focus on the derivations of $\Xi_1\left(k|\bar{g}(k),\bar{l}(k)\right)$ and $\Xi_2\left(k|\bar{g}(k),\bar{h}(k)\right)$. Because we have temporarily fixed $G_{CB}(k) = \bar{g}(k)$ and $G_{SB}(k) = \bar{l}(k)$, $P_S(k)$ can be viewed as a fixed coefficient, instead of a random variable (c.f. (1)). Therefore, to derive $\Xi(k|\bar{g}(k),\bar{h}(k),\bar{l}(k))$, we first need to determine the distribution of $Z(k) = P_C G_{CR_n}(k) + \varphi_n(k)$, which can be written as

$$F_Z(z) = \begin{cases}\frac{\bar{\varphi}\left(1-e^{-\frac{z}{\bar{\varphi}}}\right) - P_C\mu_{CR}\left(1-e^{-\frac{z}{P_C\mu_{CR}}}\right)}{\bar{\varphi}-P_C\mu_{CR}}, & \bar{\varphi}\neq P_C\mu_{CR}\\ 1-\frac{z+\bar{\varphi}}{\bar{\varphi}}e^{-\frac{z}{\bar{\varphi}}}, & \bar{\varphi}=P_C\mu_{CR}\end{cases} \tag{15}$$

Consequently, we can determine the PDF of $Z(k)$ by

$$f_Z(z) = \frac{\mathrm{d}F_Z(z)}{\mathrm{d}z} = \begin{cases}\frac{e^{-\frac{z}{\bar{\varphi}}} - e^{-\frac{z}{P_C\mu_{CR}}}}{\bar{\varphi}-P_C\mu_{CR}}, & \bar{\varphi}\neq P_C\mu_{CR}\\ \frac{z}{\bar{\varphi}^2}e^{-\frac{z}{\bar{\varphi}}}, & \bar{\varphi}=P_C\mu_{CR}\end{cases} \tag{16}$$

Denoting $W(k) = G_{SR_n}(k)/Z(k)$, we further determine the CDF of $W(k)$ by

$$F_W(w) = 1 - \frac{\mu_{SR}^2}{(\mu_{SR}+P_C\mu_{CR}w)(\mu_{SR}+\bar{\varphi}w)}. \tag{17}$$

Subsequently, by (4) and (17), it is straightforward to obtain

$$\Xi_1(k|\bar{g}(k),\bar{l}(k)) = 1 - \frac{P_S^2(k)\mu_{SR}^2}{(P_S(k)\mu_{SR}+P_C\mu_{CR}s)(P_S(k)\mu_{SR}+\bar{\varphi}s)}. \tag{18}$$

Then, by (2), (6) and (13), $\Xi_2(k|\bar{g}(k),\bar{h}(k))$ can be written and reduced to (19), where $\mathbb{E}\{\cdot\}$ denotes the expectation of the argument. Subsequently, substituting (18) and (19) into (14) yields the expression of $\Xi(k|\bar{g}(k),\bar{h}(k),\bar{l}(k))$.

A. Bulk Selection

Subsequently, by order statistics and (8), we can obtain the conditional *a posteriori* outage probability for bulk selection and reduce it by the binomial theorem to be

$$\begin{aligned}P_{out}(s|\bar{\mathbf{g}},\bar{\mathbf{h}},\bar{\mathbf{l}}) &= \left[1-\prod_{k=1}^{K}(1-\Xi(k|\bar{g}(k),\bar{h}(k),\bar{l}(k)))\right]^N\\ &= \sum_{n=0}^{N}\binom{N}{n}(-1)^n\prod_{k=1}^{K}(1-\Xi(k|\bar{g}(k),\bar{h}(k),\bar{l}(k)))^n.\end{aligned} \tag{20}$$

where $\bar{\mathbf{g}} = \{\bar{g}(1),\bar{g}(2),\ldots,\bar{g}(K)\}$, $\bar{\mathbf{h}} = \{\bar{h}(1),\bar{h}(2),\ldots,\bar{h}(K)\}$ and $\bar{\mathbf{l}} = \{\bar{l}(1),\bar{l}(2),\ldots,\bar{l}(K)\}$; $\binom{\cdot}{\cdot}$ represents the binomial coefficient. To remove the conditions and obtain the final expression, we have to average $P_{out}(s|\bar{\mathbf{g}},\bar{\mathbf{h}},\bar{\mathbf{l}})$ over $\bar{\mathbf{g}}$, $\bar{\mathbf{h}}$ and $\bar{\mathbf{l}}$, which will result in a $3K$-fold integral and can be written as

$$\begin{aligned}P_{out}(s) &= \iiint_{\bar{\mathbf{g}},\bar{\mathbf{h}},\bar{\mathbf{l}}} P_{out}(s|\bar{\mathbf{g}},\bar{\mathbf{h}},\bar{\mathbf{l}})f_{\bar{\mathbf{G}}}(\bar{\mathbf{g}})f_{\bar{\mathbf{H}}}(\bar{\mathbf{h}})f_{\bar{\mathbf{L}}}(\bar{\mathbf{l}})\mathrm{d}\bar{\mathbf{g}}\mathrm{d}\bar{\mathbf{h}}\mathrm{d}\bar{\mathbf{l}}\\ &= \sum_{n=0}^{N}\binom{N}{n}(-1)^n\left(\prod_{k=1}^{K}\Phi(k)\right),\end{aligned} \tag{21}$$

where

$$f_{\bar{\mathbf{G}}}(\bar{\mathbf{g}}) = \prod_{k=1}^{K}f_{G_{CB}}(\bar{g}(k)) = \left(\frac{1}{\mu_{CB}}\right)^K\prod_{k=1}^{K}e^{-\frac{\bar{g}(k)}{\mu_{CB}}}, \tag{22}$$

$$f_{\bar{\mathbf{H}}}(\bar{\mathbf{h}}) = \prod_{k=1}^{K}f_{G_{CD}}(\bar{h}(k)) = \left(\frac{1}{\mu_{CD}}\right)^K\prod_{k=1}^{K}e^{-\frac{\bar{h}(k)}{\mu_{CD}}}, \tag{23}$$

$$\Xi_2(k|\bar{g}(k),\bar{h}(k)) = \mathbb{P}\left\{G_{R_nD}(k) < \frac{P_C\bar{h}(k)s}{P_{R_n}(k)}\right\} = \underset{P_{R_n}(k)}{\mathbb{E}}\left\{F_{G_{RD}}\left(\frac{P_C\bar{h}(k)s}{P_{R_n}(k)}\right)\right\}$$
$$= 1 - e^{-\frac{P_C\bar{h}(k)s}{P_R\mu_{RD}}}\left[1 - e^{-\frac{(1-\alpha)P_C\bar{g}(k)}{P_R\mu_{RB}\xi}} + \frac{(1-\alpha)\mu_{RD}\bar{g}(k)e^{-\frac{(1-\alpha)P_C\bar{g}(k)}{P_R\mu_{RB}\xi}}}{(1-\alpha)\mu_{RD}\bar{g}(k) + \mu_{RB}\bar{h}(k)\xi s}\right] \tag{19}$$

and

$$f_{\bar{\mathbf{L}}}(\bar{\mathbf{l}}) = \prod_{k=1}^{K} f_{G_{SB}}(\bar{l}(k)) = \left(\frac{1}{\mu_{SB}}\right)^K \prod_{k=1}^{K} e^{-\frac{\bar{l}(k)}{\mu_{SB}}}, \tag{24}$$

denoting the joint PDFs corresponding to $\bar{\mathbf{g}}$, $\bar{\mathbf{h}}$ and $\bar{\mathbf{l}}$, respectively; $\Phi(k)$ is a triple integral, which is defined and simplified by the multinomial theorem as follows [34]:

$$\begin{aligned}\Phi(k) &= \iiint_{\bar{g},\bar{h},\bar{l}} (1 - \Xi(k|\bar{g},\bar{h},\bar{l}))^n f_{G_{CB}}(\bar{g}) f_{G_{CD}}(\bar{h}) f_{G_{SB}}(\bar{l}) \mathrm{d}\bar{g}\mathrm{d}\bar{h}\mathrm{d}\bar{l} \\ &= \iiint_{\bar{g},\bar{h},\bar{l}} \sum_{\mathsf{C}(n,4)} \frac{n!(-1)^{n_2+n_3}}{\prod_{\tau=1}^{4} n_\tau!} \Xi_1(k|\bar{g},\bar{l})^{n_2+n_4} \Xi_2(k|\bar{g},\bar{h})^{n_3+n_4} \\ &\quad \times f_{G_{CB}}(\bar{g}) f_{G_{CD}}(\bar{h}) f_{G_{SB}}(\bar{l}) \mathrm{d}\bar{g}\mathrm{d}\bar{h}\mathrm{d}\bar{l},\end{aligned} \tag{25}$$

where $\mathsf{C}(n,T) = \left\{n_1, n_2, \ldots, n_T | \sum_{\tau=1}^{T} n_\tau = n,\ \forall\ 0 \le n_\tau \le n\right\}$, denoting the executive condition of the summation operation; $\bar{g}$, $\bar{h}$ and $\bar{l}$ are the shorthand notations of variables of integration $\bar{g}(k)$, $\bar{h}(k)$ and $\bar{l}(k)$, as all subcarriers are statistically equivalent. Then, we can utilize the interchangeability between summation and integration operations and the independence among $\bar{g}$, $\bar{h}$ and $\bar{l}$ to further reduce $\Phi(k)$ to

$$\begin{aligned}\Phi(k) &= \sum_{\mathsf{C}(n,4)} \frac{n!(-1)^{n_2+n_3}}{\prod_{\tau=1}^{4} n_\tau!} \\ &\quad \times \int_0^\infty \phi_1(k, n_2+n_4)\phi_2(k, n_3+n_4) f_{G_{CB}}(\bar{g})\mathrm{d}\bar{g},\end{aligned} \tag{26}$$

where

$$\phi_1(k,n) = \int_0^\infty \Xi_1(k|\bar{g},\bar{l})^n f_{G_{SB}}(\bar{l})\mathrm{d}\bar{l}, \tag{27}$$

and

$$\phi_2(k,n) = \int_0^\infty \Xi_2(k|\bar{g},\bar{h})^n f_{G_{CD}}(\bar{h})\mathrm{d}\bar{h}. \tag{28}$$

Now, let us focus on the derivations of $\phi_1(k, n_2+n_4)$ and $\phi_2(k, n_3+n_4)$. For $\phi_1(k, n_2+n_4)$, we can similarly employ the binomial theorem and obtain

$$\phi_1(k, n_2+n_4) = \sum_{p=0}^{n_2+n_4} \binom{n_2+n_4}{p} (-1)^p \vartheta(k), \tag{29}$$

where $\vartheta(k)$ is determined in (30); $\chi_u^{(p)}(\mathbf{a}, b)$ is a defined function given by

$$\chi_u^{(p)}(\mathbf{a}, b) = \int_u^\infty \frac{e^{-bx}}{\prod_{\mathbf{a}}(x+a_i)^p}\mathrm{d}x, \tag{31}$$

where $\mathbf{a} = \{a_1, a_2, \ldots, a_{N_a}\}$ denotes a set of N_a positive numbers; b and u are positive numbers; p is a nonnegative integer. When $p = 0$, we can easily obtain

$$\chi_u^{(0)}(\mathbf{a}, b) = e^{-bu}/b. \tag{32}$$

When $p > 0$, by partial fraction decomposition [35], we can determine the closed-form expression of $\chi_u^{(p)}(\mathbf{a}, b)$ by

$$\begin{aligned}\chi_u^{(p)}(\mathbf{a}, b) &= \int_u^\infty \sum_{q=1}^{p} \sum_{i=1}^{N_a} \left[\frac{A(q,i)}{(x+a_i)^q}\right] e^{-bx}\mathrm{d}x \\ &= \sum_{q=1}^{p} \sum_{i=1}^{N_a} A(q,i) \int_u^\infty \frac{e^{-bx}}{(x+a_i)^q}\mathrm{d}x \\ &= \sum_{q=1}^{p} \sum_{i=1}^{N_a} A(q,i) e^{a_i b} \Gamma\left(1-q, b(a_i+u)\right),\end{aligned} \tag{33}$$

where $\{A(q,i)\}$ is a unique and real constant set, which can be derived by a recursive algorithm for any given $\mathbf{a}$ and p [36]; $\Gamma(a,x) = \int_x^\infty t^{a-1}e^{-t}\mathrm{d}t$ is the incomplete gamma function.

For $\phi_2(k, n_3+n_4)$, we can derive its closed-form expression by applying the binomial theorem twice and exchanging the order of summation and integration, and obtain

$$\begin{aligned}&\phi_2(k, n_3+n_4) \\ &= \sum_{p=0}^{n_3+n_4} \sum_{q=0}^{p} \binom{n_3+n_4}{p} \binom{p}{q} (-1)^p \left[1 - e^{-\frac{(1-\alpha)P_C\bar{g}}{P_R\mu_{RB}\xi}}\right]^{p-q} \theta(k),\end{aligned} \tag{34}$$

where $\theta(k)$ is defined and reduced to (35). Consequently, by substituting the single integral expression of $\Phi(k)$ into (21), we can reduce $P_{out}(s)$ from a $3K$-fold integral to a summation of multiplications of a series of single integrals, which can be easily evaluated by standard numerical approaches. However, to the best of the authors' knowledge, there does not exist a closed-form expression of $P_{out}(s)$ when the dynamic power control mechanism is applied.

In addition, because of the demanding estimation of instantaneous channel state information (CSI), the BS might not always be able to get access to $\bar{g}$, and therefore a static power control mechanism will be applied in this scenario. Specifically, the static power control mechanism will not take $\bar{g}$ into account, but replace it with a preset static power control factor[7] κ, which is determined by the statistical features of the network [37]. Then, we can derive the closed-form expression of outage probability in (36) for bulk selection. Though useful, the expression is still complicated and it is not easy to observe the relations among outage performance and system parameters, as $\phi_1(k,n)$ and $\phi_2(k,n)$ are involved. To further simplify the expression and provide an insight into the

[7]One should note that the static power control mechanism cannot always eliminate the deleterious effects of the interference from D2D communications to cellular communications. Although it could bring a better outage performance to D2D communications by releasing power control, this performance gain at the D2D side is at the price of the performance loss of cellular communications [37]. As a consequence, the higher κ is, the better the outage performance in D2D communications will be, and vice versa. In other words, this provides a performance trade-off between cellular communications and D2D communications, when both coexist in an underlay manner.

$$\begin{aligned}\vartheta(k) &= \int_0^\infty \left[\frac{P_S^2(k)\mu_{SR}^2}{(P_S(k)\mu_{SR}+P_C\mu_{CR}s)(P_S(k)\mu_{SR}+\bar{\varphi}s)}\right]^p f_{G_{SB}}(\bar{l})\mathrm{d}\bar{l} \\ &= \left(1-e^{-\frac{\alpha P_C\bar{g}}{\bar{P}_S\mu_{SB}\xi}}\right)\left[\frac{\bar{P}_S^2\mu_{SR}^2}{(\bar{P}_S\mu_{SR}+P_C\mu_{CR}s)(\bar{P}_S\mu_{SR}+\bar{\varphi}s)}\right]^p + \frac{1}{\mu_{SB}}\left(\frac{\alpha^2P_C\bar{g}^2\mu_{SR}^2}{\mu_{CR}\bar{\varphi}\xi^2s^2}\right)^p \chi^{(p)}_{\frac{\alpha P_C\bar{g}}{\bar{P}_S\xi}}\left(\left\{\frac{\alpha\bar{g}\mu_{SR}}{\mu_{CR}\xi s}, \frac{\alpha P_C\bar{g}\mu_{SR}}{\bar{\varphi}\xi s}\right\}, \frac{1}{\mu_{SB}}\right)\end{aligned} \tag{30}$$

$$\begin{aligned}\theta(k) &= \int_0^\infty \left[\frac{(1-\alpha)\mu_{RD}\bar{g}e^{-\frac{(1-\alpha)P_C\bar{g}}{\bar{P}_R\mu_{RB}\xi}}}{(1-\alpha)\mu_{RD}\bar{g}+\mu_{RB}\bar{h}\xi s}\right]^q e^{-\left(\frac{pP_Cs}{\bar{P}_R\mu_{RD}}+\frac{1}{\mu_{CD}}\right)\bar{h}}\mathrm{d}\bar{h} \\ &= \left[\frac{(1-\alpha)\mu_{RD}\bar{g}e^{-\frac{(1-\alpha)P_C\bar{g}}{\bar{P}_R\mu_{RB}\xi}}}{\mu_{RB}\xi s}\right]^q \left(\frac{pP_Cs}{\bar{P}_R\mu_{RD}}+\frac{1}{\mu_{CD}}\right)^{q-1} e^{\frac{(1-\alpha)\mu_{RD}\bar{g}}{\mu_{RB}\xi s}\left(\frac{pP_Cs}{\bar{P}_R\mu_{RD}}+\frac{1}{\mu_{CD}}\right)}\Gamma\left(1-q, \frac{(1-\alpha)\mu_{RD}\bar{g}}{\mu_{RB}\xi s}\left(\frac{pP_Cs}{\bar{P}_R\mu_{RD}}+\frac{1}{\mu_{CD}}\right)\right)\end{aligned} \tag{35}$$

$$P_{out}(s) = \sum_{n=0}^{N}\binom{N}{n}(-1)^n\prod_{k=1}^{K}\left[\sum_{\mathsf{C}(n,4)}\left(\frac{n!(-1)^{n_2+n_3}}{\prod_{\tau=1}^{4}n_\tau!}\phi_1(k,n_2+n_4)|_{\bar{g}=\kappa}\phi_2(k,n_3+n_4)|_{\bar{g}=\kappa}\right)\right] \tag{36}$$

proposed system, we release the hardware constraints on transmit power at DUE transmitter and relays and assume the residual SI to be eliminated by advanced SI cancellation technologies. Then, mathematically, we have $\bar{P}_S \to \infty$, $\bar{P}_R \to \infty$ and $\bar{\varphi} \to 0$. Consequently, we can derive the outage floor in a neat expression for relay-assisted OFDM D2D systems applying bulk selection and static power control mechanism by

$$\tilde{P}_{out} = \sum_{n=0}^{N}\binom{N}{n}(-1)^n\left[\mathscr{E}_n\left(\frac{\alpha\mu_{SR}\kappa}{\mu_{SB}\mu_{CR}\xi s}\right)\mathscr{E}_n\left(\frac{(1-\alpha)\mu_{RD}\kappa}{\mu_{RB}\mu_{CD}\xi s}\right)\right]^K, \tag{37}$$

where $\mathscr{E}_n(x) = xe^xE_n(x)$ and $E_n(x) = \int_1^\infty e^{-xt}/t^n\mathrm{d}t$ denotes the exponential integral function.

By (37), the potential of the proposed relay-assisted OFDM D2D system in idealized conditions can be shown, and the relations among outage performance and system parameters are revealed. Meanwhile, it can be observed that the symmetry between channels for a certain subcarrier in the first and second hops is only related to the power coordination factor α. Also, because of the summation over multiple terms with opposite signs, increasing the number of relays N might not be an efficient way to enhance outage performance when applying bulk selection.

B. Per-Subcarrier Selection

Similarly, by (9), we can derive the conditional *a posteriori* outage probability for per-subcarrier selection to be

$$P_{out}(s|\bar{\mathbf{g}},\bar{\mathbf{h}},\bar{\mathbf{l}}) = 1-\prod_{k=1}^{K}\left[1-\left(\Xi(k|\bar{g},\bar{h},\bar{l})\right)^N\right]. \tag{38}$$

In a similar manner as bulk selection, we remove the conditions by averaging $P_{out}(s|\bar{\mathbf{g}},\bar{\mathbf{h}},\bar{\mathbf{l}})$ over $\bar{\mathbf{g}}$, $\bar{\mathbf{h}}$ and $\bar{\mathbf{l}}$, which leads to a $3K$-fold integral and can be expressed as

$$\begin{aligned}P_{out}(s) &= \iiint_{\bar{\mathbf{g}},\bar{\mathbf{h}},\bar{\mathbf{l}}} P_{out}(s|\bar{\mathbf{g}},\bar{\mathbf{h}},\bar{\mathbf{l}})f_{\bar{\mathbf{G}}}(\bar{\mathbf{g}})f_{\bar{\mathbf{H}}}(\bar{\mathbf{h}})f_{\bar{\mathbf{L}}}(\bar{\mathbf{l}})\mathrm{d}\bar{\mathbf{g}}\mathrm{d}\bar{\mathbf{h}}\mathrm{d}\bar{\mathbf{l}} \\ &= 1-\prod_{k=1}^{K}\left(1-\Psi(k)\right),\end{aligned} \tag{39}$$

where $\Psi(k)$ is defined and can be simplified by the multinomial theorem as follows [34]:

$$\begin{aligned}\Psi(k) &= \iiint_{\bar{g},\bar{h},\bar{l}}\left(\Xi(k|\bar{g},\bar{h},\bar{l})\right)^N f_{G_{CB}}(\bar{g})f_{G_{CD}}(\bar{h})f_{G_{SB}}(\bar{l})\mathrm{d}\bar{g}\mathrm{d}\bar{h}\mathrm{d}\bar{l} \\ &= \iiint_{\bar{g},\bar{h},\bar{l}}\sum_{\mathsf{C}(N,3)}\frac{N!(-1)^{n_3}}{\prod_{\tau=3}^{3}n_\tau!}\Xi_1(k|\bar{g},\bar{l})^{n_1+n_3}\Xi_2(k|\bar{g},\bar{h})^{n_2+n_3} \\ &\quad\times f_{G_{CB}}(\bar{g})f_{G_{CD}}(\bar{h})f_{G_{SB}}(\bar{l})\mathrm{d}\bar{g}\mathrm{d}\bar{h}\mathrm{d}\bar{l}.\end{aligned} \tag{40}$$

Because of the interchangeability between summation and integration operations and the independence among $\bar{g}$, $\bar{h}$ and $\bar{l}$, we can simplify the triple integral in $\Psi(k)$ to a summation of a series of single integrals as

$$\begin{aligned}\Psi(k) = &\sum_{\mathsf{C}(N,3)}\frac{N!(-1)^{n_3}}{\prod_{\tau=1}^{3}n_\tau!} \\ &\times\int_0^\infty\phi_1(k,n_1+n_3)\phi_2(k,n_2+n_3)f_{G_{CB}}(\bar{g})\mathrm{d}\bar{g}.\end{aligned} \tag{41}$$

Finally, substituting (41) into (39) yields the single integral expression of the outage probability for per-subcarrier selection when the dynamic power control mechanism is applied. Again, if the static power control mechanism is applied, we can express the closed-form expression of outage probability for per-subcarrier selection in (42). To provide an insight into systems applying per-subcarrier selection and static power control mechanism, we can simplify (42) by assuming $\bar{P}_S \to \infty$, $\bar{P}_R \to \infty$ and $\bar{\varphi} \to 0$ and obtain the outage floor in a neat expression as

$$\begin{aligned}\tilde{P}_{out}(s) = 1-\Bigg[1-\sum_{n=0}^{N}\binom{N}{n}(-1)^n&\mathscr{E}_n\left(\frac{\alpha\mu_{SR}\kappa}{\mu_{SB}\mu_{CR}\xi s}\right) \\ &\times\mathscr{E}_n\left(\frac{(1-\alpha)\mu_{RD}\kappa}{\mu_{RB}\mu_{CD}\xi s}\right)\Bigg]^K.\end{aligned} \tag{43}$$

By (43), the potential of the per-subcarrier selection in relay-assisted OFDM D2D networks under these two idealized conditions can be quantified. Similarly, the symmetry between two

$$P_{out}(s) = 1 - \prod_{k=1}^{K} \left[1 - \sum_{\mathsf{C}(N,3)} \left(\frac{N!(-1)^{n_3}}{\prod_{\tau=1}^{3} n_\tau!} \phi_1(k, n_1+n_3)|_{\bar{g}=\kappa} \phi_2(k, n_2+n_3)|_{\bar{g}=\kappa} \right) \right] \tag{42}$$

hops is also only related to the power coordination factor α and the number of subcarriers K has a great impact on the outage performance.

IV. Outage Performance Optimization

Because of the joint power control mechanism at DUE transmitter and relays, there exists a trade-off of α in the outage performance of relay-assisted D2D communications, which is associated with channel statistics. That is to say, there exists an optimal $\alpha^* \in (0,1)$, which is capable of minimizing the outage probability. Following this thought, we can then formulate an outage performance optimization problem infra

$$\begin{aligned} &\min_{\alpha} \{P_{out}(s)\} \\ &\text{s.t. } 0 < \alpha < 1. \end{aligned} \tag{44}$$

Because all subcarriers are statistically equivalent, this formulated optimization problem can be equivalently transfered to an optimization problem of maximizing the average end-to-end SIR regarding an individual subcarrier, written as

$$\begin{aligned} &\max_{\alpha} \{\mathbb{E}\{\Gamma_{SR_nD}(k)\}\} \\ &\text{s.t. } 0 < \alpha < 1. \end{aligned} \tag{45}$$

The equivalence of these two optimization problems can be proved in a general manner in Appendix A.

A. Dynamic Power Control Mechanism

Because $\mathbb{E}\{\Gamma_{SR_nD}(k)\}$ is mathematically intractable, we must find another alternative objective function to approximate $\mathbb{E}\{\Gamma_{SR_nD}(k)\}$ and provide a suboptimal solution instead. Therefore, for the dynamic power control mechanism, we formulate an alternative optimization problem to approximate the original problem formulated in (45) by

$$\begin{aligned} &\max_{\alpha} \{\Omega(\alpha)\} \\ &\text{s.t. } 0 < \alpha < 1, \end{aligned} \tag{46}$$

where $\Omega(\alpha)$ is constructed by replacing all instantaneous channel power gains by their averages in $\Gamma_{SR_nD}(k)$ except for $\bar{g}(k)$, and averaging over $\bar{g}(k)$; $\Omega(\alpha)$ can be explicitly expressed in (47). Then, we prove the quasi-concavity of the formulated problem in Appendix B, which enables it to be efficiently solved by standard optimization techniques (e.g. CVX in MATLAB [38]), and a suboptimal $\alpha^{\&}$ can be yielded to improve the outage performance when the dynamic power control mechanism is applied.

B. Static Power Control Mechanism

Again, because it is difficult to analyze $\mathbb{E}\{\Gamma_{SR_nD}(k)\}$ directly, we propose an alternative optimization problem for the static power control case. This new optimization problem can be written as

$$\begin{aligned} &\max_{\alpha} \{\gamma(\alpha)\} \\ &\text{s.t. } 0 < \alpha < 1, \end{aligned} \tag{48}$$

where $\gamma(\alpha) = \min\{\gamma_1(\alpha), \gamma_2(\alpha)\}$; $\gamma_1(\alpha)$ and $\gamma_2(\alpha)$ are given below:

$$\gamma_1(\alpha) = \frac{\mu_{SR} \min\left\{\frac{\alpha P_C \kappa}{\xi \mu_{SB}}, \bar{P}_S\right\}}{P_C \mu_{CR} + \bar{\varphi}}, \tag{49}$$

and

$$\gamma_2(\alpha) = \frac{\mu_{RD} \min\left\{\frac{(1-\alpha) P_C \kappa}{\xi \mu_{RB}}, \bar{P}_R\right\}}{P_C \mu_{CD}}, \tag{50}$$

which are produced by replacing all instantaneous channel power gains in $\Gamma_{SR_nD}(k)$ by their averages. Subsequently, we can prove this alternative optimization problem to be quasi-concave in Appendix C. As a result, this optimization problem can be efficiently solved by using standard optimization techniques, and a suboptimal $\alpha^{\&}$ can be yielded to improve the outage performance when the static power control mechanism is applied.

V. Numerical Results

A. Verifications of Analytical Results

To verify the analysis presented in Section III for different relay selection schemes and power control mechanisms, we carried out Monte Carlo simulations in this section. First, we set $\mu_{SR} = \mu_{RD} = 30$ dB, $\mu_{SB} = \mu_{RB} = 10$ dB, $\mu_{CR} = \mu_{CD} = 2$ dB, $\mu_{CB} = 20$ dB and $\bar{\varphi} = 5$ dB[8]; also, we normalize $s = \xi = P_C = 1$ and let $\alpha = 0.5$ (without considering power coordination for the time being) and $\kappa = 4$ for implementing the static power control mechanism. We further suppose $\bar{P}_R = \bar{P}_S$ and vary this transmit power limit to substantiate (21), (36), (39) and (42). The simulation results are shown in Fig. 3 for bulk and per-subcarrier selection schemes with different numbers of subcarriers and relays.

From Fig. 3, we can see that the theoretical results perfectly match the numerical results, which validate the correctness of our analysis given in Section III. In addition, the per-subcarrier selection scheme outperforms the bulk selection scheme in terms of outage probability when $\bar{P}_S$ and $\bar{P}_R$ are small. However, with the increase of $\bar{P}_S$ and $\bar{P}_R$, outage probabilities corresponding to both selection schemes get close when dynamic power control mechanism is applied, which indicates that the dynamic power control mechanism dominates the outage performance as long as $\bar{P}_S$ and $\bar{P}_R$ are sufficiently large, instead of relay selections. On the contrary, this is not the case for the static power control

[8]The practical values of these parameters are relevant to a number of factors, e.g. network topology, system configuration and noise etc. Considering the generality, simulation parameters have been normalized in this paper, and the average channel gains chosen for simulations in this paper are only relative. The representative set of the average channel gains is typical. The reasons for choosing these values are explained as follows. For the average channel gains for transmission channels, i.e. μ_{SR} and μ_{RD}, they should be much larger than the average gains of other channels, otherwise, D2D transmission would not be preferable in such a scenario. Then, the channel between source and BS and the channel between relay and BS should be relatively stronger, which justify the necessity of power control. The signals from other channels are treated as interference, which are thus relatively small and have a similar level. Similar normalization-based methods for choosing simulation parameters are commonly adopted by research works related to D2D communications [8], [11], [14], [18].

$$\Omega(\alpha)=\mathop{\mathbb{E}}_{\bar{g}(k)}\left\{\min\left\{\frac{\mu_{SR}\min\left\{\frac{\alpha P_C\bar{g}(k)}{\xi\mu_{SB}},\bar{P}_S\right\}}{P_C\mu_{CR}+\bar{\varphi}},\frac{\mu_{RD}\min\left\{\frac{(1-\alpha)P_C\bar{g}(k)}{\xi\mu_{RB}},\bar{P}_R\right\}}{P_C\mu_{CD}}\right\}\right\}=\begin{cases}\omega_1(\alpha), & \frac{\bar{P}_S\mu_{SR}}{P_C\mu_{CR}+\bar{\varphi}}>\frac{\bar{P}_R\mu_{RD}}{P_C\mu_{CD}}\\ \omega_2(\alpha), & \frac{\bar{P}_S\mu_{SR}}{P_C\mu_{CR}+\bar{\varphi}}\le\frac{\bar{P}_R\mu_{RD}}{P_C\mu_{CD}}\end{cases} \tag{47a}$$

$$\omega_1(\alpha)=\begin{cases}\frac{\alpha P_C\mu_{SR}\mu_{CB}}{\xi\mu_{SB}(P_C\mu_{CR}+\bar{\varphi})}\left[1-e^{-\frac{\xi\bar{P}_R\mu_{SB}\mu_{RD}(P_C\mu_{CR}+\bar{\varphi})}{\alpha P_C^2\mu_{SR}\mu_{CB}\mu_{CD}}}\right], & 0<\alpha<\varrho\\ \frac{(1-\alpha)P_C\mu_{RD}\mu_{CB}}{P_C\xi\mu_{RB}\mu_{CD}}\left[1-e^{-\frac{\bar{P}_R\xi\mu_{RB}}{(1-\alpha)P_C\mu_{CB}}}\right], & \varrho\le\alpha<1\end{cases} \tag{47b}$$

$$\omega_2(\alpha)=\begin{cases}\frac{\alpha P_C\mu_{SR}\mu_{CB}}{\xi\mu_{SB}(P_C\mu_{CR}+\bar{\varphi})}\left[1-e^{-\frac{\bar{P}_S\xi\mu_{SB}}{\alpha P_C\mu_{CB}}}\right], & 0<\alpha<\varrho\\ \frac{(1-\alpha)P_C\mu_{RD}\mu_{CB}}{P_C\xi\mu_{RB}\mu_{CD}}\left[1-e^{-\frac{\bar{P}_SP_C\xi\mu_{SR}\mu_{RB}\mu_{CD}}{(1-\alpha)P_C\mu_{RD}\mu_{CB}(P_C\mu_{CR}+\bar{\varphi})}}\right], & \varrho\le\alpha<1\end{cases} \tag{47c}$$

$$\varrho=\frac{\mu_{SB}\mu_{RD}(P_C\mu_{CR}+\bar{\varphi})}{P_C\mu_{SR}\mu_{RB}\mu_{CD}+\mu_{SB}\mu_{RD}(P_C\mu_{CR}+\bar{\varphi})} \tag{47d}$$

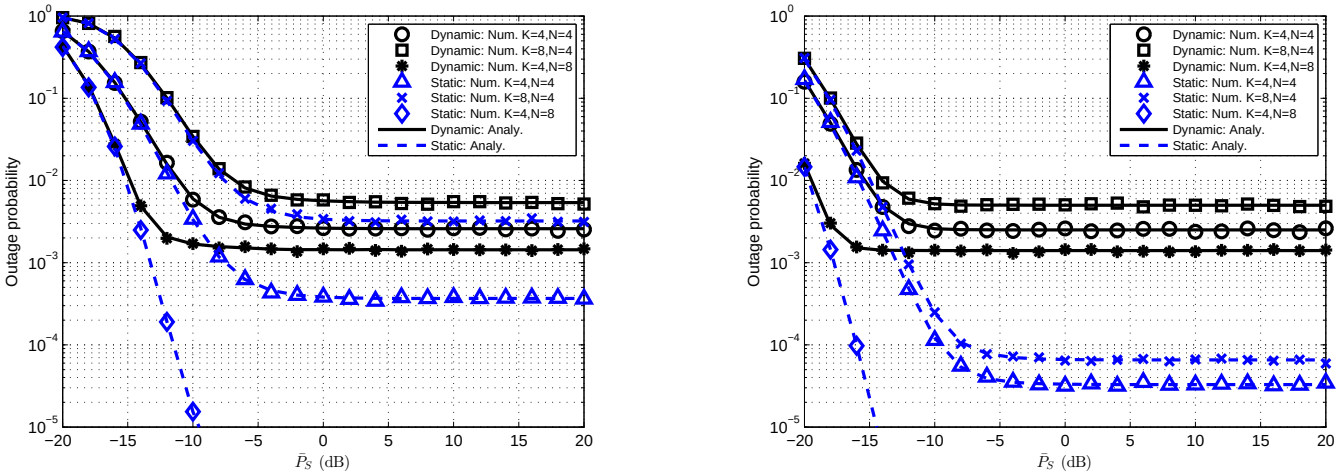

(a) Bulk selection scheme

(b) Per-subcarrier selection scheme

Fig. 3: Outage probability of D2D communications vs. $\bar{P}_S$ for bulk and per-subcarrier selection schemes, given $\bar{P}_R=\bar{P}_S$.

mechanism, as the correlation term $\bar{g}(k)$ is out of consideration, which will result in a significant performance improvement by using per-subcarrier selection.

Meanwhile, some important features of the proposed full-duplex relay-assisted OFDM D2D system can also be shown in Fig. 3. First, the power control mechanisms constraint the improvement of outage performance by increasing $\bar{P}_S$ and $\bar{P}_R$, as it is dominated by the interference to cellular communications when $\bar{P}_S$ and $\bar{P}_R$ are large. Second, both dynamic and static power control mechanisms share the similar outage performance when $\bar{P}_S$ and $\bar{P}_R$ are small, but will have a performance gap when $\bar{P}_S$ and $\bar{P}_R$ increase. The performance gap is mainly determined by the static power control factor κ. Besides, increasing the number of subcarriers K will lead to a larger outage probability, as all subcarriers have to be ensured not in outage (c.f. *Definition 1*). On the other hand, increasing the number of relays N will yield a lower outage probability, because the DUE transmitter can have more options when performing multicarrier relay selections. Moreover, the positive effect on outage performance by increasing N for the static power control mechanism is much more obvious than that for the dynamic power control mechanism, since there is one less correlation term when the static power control mechanism is applied. These results provide guidelines for the design of OFDM D2D systems, when coexisting with traditional cellular systems in an underlay manner.

B. Performance Benefits by Relay Selections and Comparisons

1) Effects of μ_{SR} and μ_{RD}: In order to study the effects of the D2D transmission links, we focus on μ_{SR} and μ_{RD} in this subsection, which are directly related to the quality of relay-assisted D2D communications. To simulate, we normalize $\bar{P}_S=\bar{P}_R=1$, set $N=K=4$, and maintain other settings as the same in the last subsection. Then, we assume $\mu_{RD}=\mu_{SR}$, and vary them to obtain the relation between the outage probability and the quality of D2D transmission links. Meanwhile, to illustrate the performance benefits brought by relay selections, we also take random relay selection as a comparison benchmark in our simulations. The numerical results are illustrated in Fig. 4. By these numerical results, it is clear that the outage performance yielded by bulk and per-subcarrier selections will get close with increasing μ_{SR} and μ_{RD} when the dynamic power control mechanism is applied, while this does not happen for

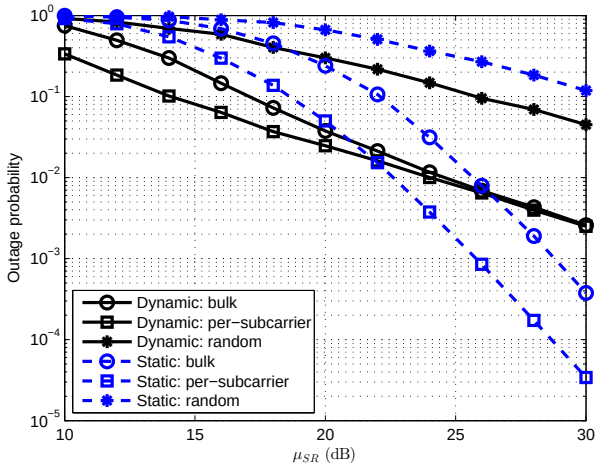

Fig. 4: Outage probability of D2D communications vs. the average channel power gain μ_{SR}, given $\mu_{RD} = \mu_{SR}$ and $N = K = 4$.

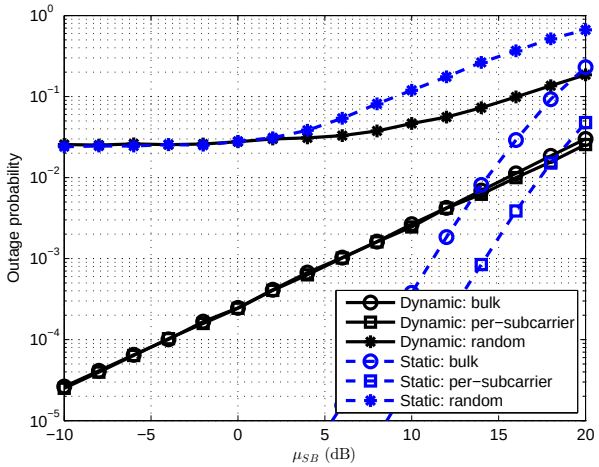

Fig. 5: Outage probability of D2D communications vs. the average channel power gain μ_{SB}, given $\mu_{RB} = \mu_{SB}$ and $N = K = 4$.

the case of static power control mechanism. This is because with increasing μ_{SR} and μ_{RD}, the outage event is dominated by the deepest fade over all subcarriers. Therefore, when the dynamic power control mechanism is applied, the relay selected to forward the deepest faded subcarrier (i.e. with the minimum SIR) will be the same by bulk and per-subcarrier selections. Furthermore, compared to the random selection scheme, both bulk and subcarrier selection schemes own outage performance gains, which validate the effectiveness of multicarrier relay selections in full-duplex relay-assisted OFDM D2D systems.

2) Effects of μ_{SB} and μ_{RB}: The channels between BS and DUE transmitter as well as relays are important, as they are related to the power control mechanisms. Here, we also investigate them via μ_{SB} and μ_{RB}. By taking a similar simulation configurations as above, and fixing $\mu_{SR} = \mu_{RD} = 30$ dB, we assume $\mu_{RB} = \mu_{SB}$, and vary them to illustrate how the qualities of these channels affect the outage performance of D2D communications. The numerical results are given in Fig. 5. We can find from this figure that increasing μ_{SB} and μ_{RB} will yield a significantly negative impact on the outage performance, because on average, less transmit power will be allowed for D2D communications when μ_{SB} and μ_{RB} go large. Meanwhile, because of the correlation term $\bar{l}(k)$, bulk and per-subcarrier selections have the similar outage performance when μ_{SR} and μ_{RD} are large.

3) Effects of μ_{CR} and μ_{CD}: Additionally, the channels between CUE and relay as well as DUE receiver determine the quality of signal reception, as the transmitted signals from CUEs are regarded as interference to relays and the DUE receiver. Here, we let $\mu_{CD} = \mu_{CR}$, and change them to observe their impacts on the D2D signal reception. The numerical results are shown in Fig. 6. The numerical results demonstrated in Fig. 6 are aligned with our expectation that increasing μ_{CR} and μ_{CD} will produce a destructive effect on outage performance, as a large interference from cellular communications will exist at relays and the DUE receiver. Meanwhile, because of the correlation term $\bar{h}(k)$, with decreasing μ_{CR} and μ_{CD}, the performance curves of bulk and per-subcarrier selections get close.

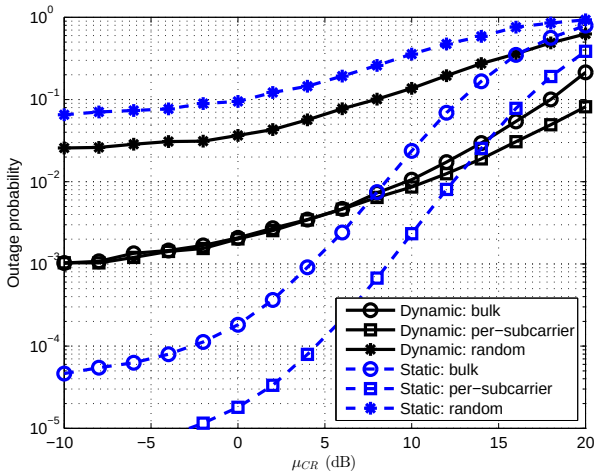

Fig. 6: Outage probability of D2D communications vs. the average channel power gain μ_{CR}, given $\mu_{CD} = \mu_{CR}$ and $N = K = 4$.

C. Comparison between Dynamic and Static Power Control Mechanisms

The performance difference between dynamic and static power control mechanisms mainly depends on μ_{CB} and κ. In this subsection, we study the relation between μ_{CB} and outage performance with different κ. To provide a comprehensive analysis of the effects of μ_{CB} on both D2D and cellular communications, we should take the outage probabilities from both sides into consideration. Taking the same simulation configurations specified in Section V-A and normalizing $\bar{P}_S = \bar{P}_R = 1$, we carry out the numerical simulations and present the numerical results in Fig. 7 for both D2D and cellular communications.

From Fig. 7 (a), we can observe that the outage probabilities regarding bulk and per-subcarrier selections get close at high μ_{CB}, which indicates that the correlation term $\bar{g}(k)$ plays a dominant role in the relay selection process, and produces a deleterious impact on the performance gain. This sub-figure also provides a hint to choose appropriate power control mechanisms. Meanwhile, when the static power control mechanism is applied, a lower κ

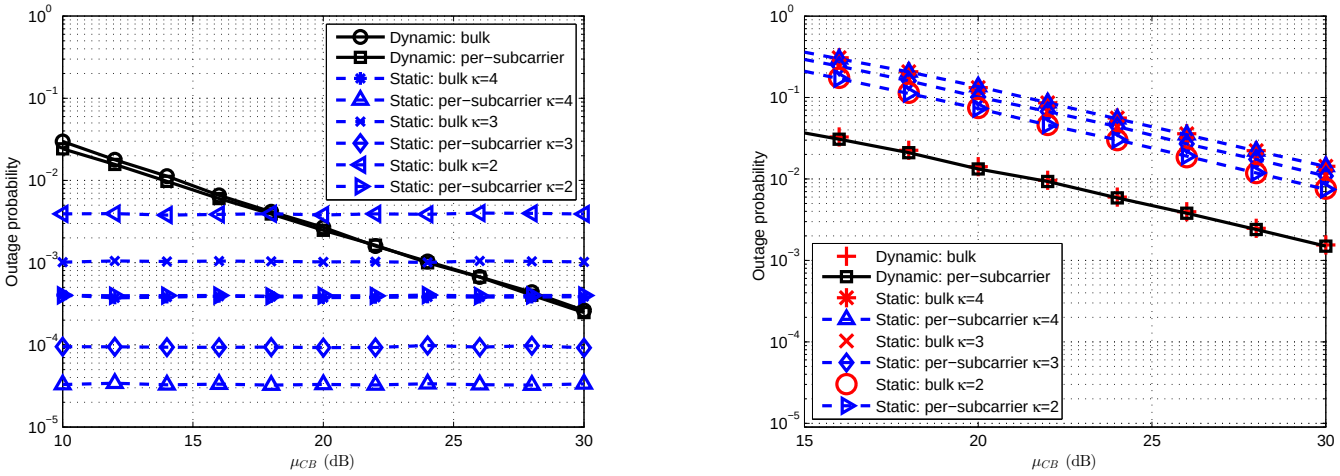

(a) D2D communications

(b) Cellular communications

Fig. 7: Outage probability vs. μ_{CB} for D2D and cellular communications, given $N = K = 4$.

will lead to a lower outage probability, and the performance is independent from μ_{CB}, as $\bar{g}(k)$ is not taken into consideration for static power control. On the other hand, by observing Fig. 7 (b), the numerical results verify our analysis that the potential performance gain in D2D communications brought by the static power control mechanism is at the price of the performance loss in cellular communications. Besides, as we can also see, the relay selection schemes adopted by DUEs does not matter to the cellular communications, because on average, all relays are viewed equivalently to the BS, and so is their interference.

D. Comparison between Full-Duplex and Half-Duplex Transmissions

As it is well known that full-duplex transmission does not always outperform half-duplex transmission [39], the performance difference between them is mainly dependent on the average power of the residual SI term, i.e. $\bar{\varphi}$. Therefore, we study $\bar{\varphi}$ in this subsection and compare the outage performance provided by full-duplex and half-duplex transmissions (c.f. (10) and (11)). Meanwhile, we also provide an ideal case that the power of residual SI can be mitigated to a noise level and is thus negligible to show the ideal scenario of full-duplex transmission for comparison purposes. This ideal case can be produced by

$$P_{out}^{ideal}(s) = \lim_{\bar{\varphi}\to 0} P_{out}(s). \tag{51}$$

Taking the same simulation configurations given in Section V-A and normalizing $\bar{P}_S = \bar{P}_R = 1$, we carry out the numerical simulations and all simulation results are shown in Fig. 8. From this figure, it is obvious that the priority of transmission protocols depends on $\bar{\varphi}$, and full-duplex transmission does have the potential to provide a lower outage probability, as long as a satisfactory SI elimination technology can be utilized to reduce $\bar{\varphi}$ below a certain level. The analytical derivation of the critical value of $\bar{\varphi}$ below which the full-duplex transmission outperforms the half-duplex transmission (i.e. the cross point of two outage probability curves) would be worth investigating as a future work.

E. Verifications of Outage Performance Optimization Strategies

To verify the effectiveness of the suboptimal solutions to the original optimization problem formulated in (44), we carry out simulations to investigate the relation between α and outage probability in this subsection. Here we adopt the same simulation configurations as set in Section V-A and normalize $\bar{P}_S = \bar{P}_R = 1$. Simulation results are shown in Fig. 9. Compared with the optimal[9] and suboptimal power coordination factors α^* and $\alpha^{\&}$ (highlighted by red circles and blue squares), our proposed suboptimal solutions are close to the optimal solutions, which validate the feasibility of our proposed suboptimal algorithms for both dynamic and static power control cases. Therefore, we can employ these algorithms to efficiently coordinate transmit power among DUE transmitter and relays to yield a lower outage probability.

VI. Conclusion

In this paper, we proposed an underlay OFDM D2D system, which is assisted by multiple full-duplex DF relays, and considered applying multicarrier relay selections in this system. Meanwhile, power control mechanisms and performance optimizations were also taken into consideration in order to efficiently mitigate the interference from D2D communications to cellular communications. Then, we analyzed the outage performance of the proposed system. We obtained the single integral expressions of the outage probabilities when the dynamic power control mechanism was applied, and these expressions can be further simplified to closed forms when the static power control mechanism was utilized. Meanwhile, by assuming two ideal conditions, the outage floors for the static power control mechanism were derived in neat and closed forms, which clearly reveal the relations among outage performance and system parameters. After that, we studied the outage performance optimization problem by coordinating transmit power among DUE transmitter and relays. Due to the mathematical intractability of the original optimization problem, we proposed

[9]Here, the optimal α^* in simulations is produced by a brute-force method searching over the full set of α with a small increment from zero to one.

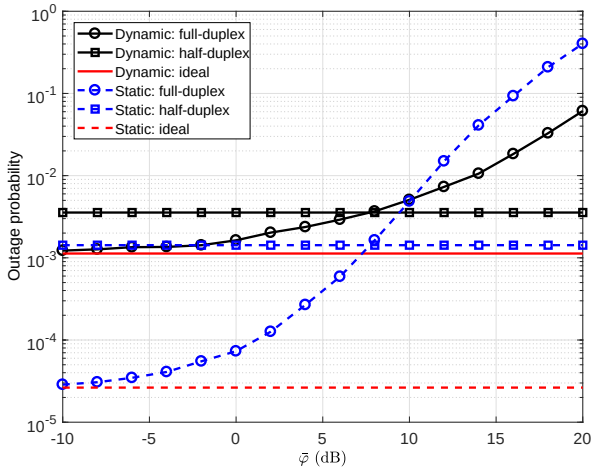

(a) Bulk selection scheme

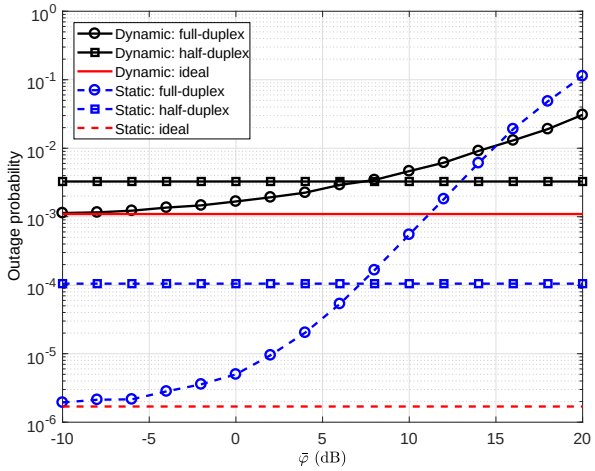

(b) Per-subcarrier selection scheme

Fig. 8: Outage probability of D2D communications vs. $\bar{\varphi}$ for bulk and per-subcarrier selection schemes, given $N = K = 4$.

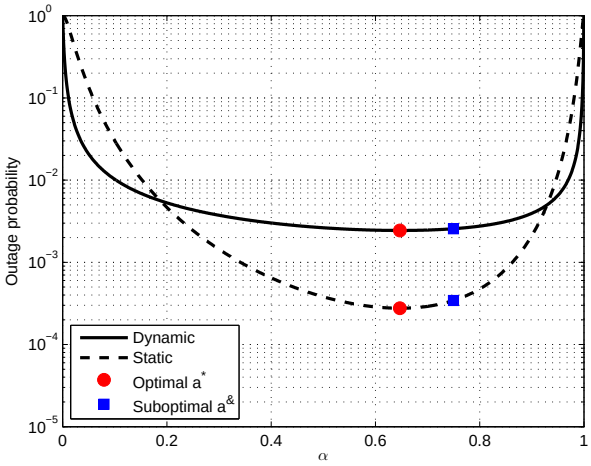

(a) Bulk selection scheme

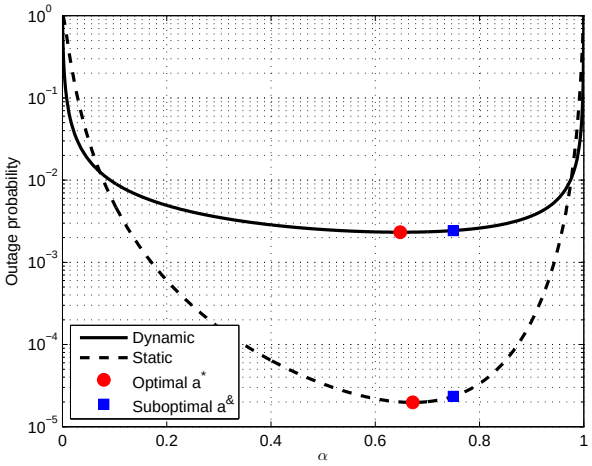

(b) Per-subcarrier selection scheme

Fig. 9: Outage probability of D2D communications vs. α for bulk and per-subcarrier selection schemes, given $N = K = 4$.

two alternative optimization problems, which are capable of providing suboptimal solutions for both dynamic and static power control cases. By the analytical and numerical results provided in this paper, we can have an insight into the relay-assisted OFDM D2D system, and understand its characteristics in most aspects thoroughly. Moreover, as a number of comparisons are given, this paper can also provide a guideline for implementing D2D communications and the relevant technologies in next generation networks.

Appendix A
Proof of Equivalence of Optimization Problems Formulated in (44) and (45)

According to the theorem of Lebesgue-Stieltjes integration, for an arbitrary random variable X with CDF $F_X(x)$, we can derive its expectation as follows [40]:

$$\mathbb{E}\{X\} = \int_0^{\infty} (1 - F_X(x))\mathrm{d}x - \int_{-\infty}^{0} F_X(x)\mathrm{d}x. \tag{52}$$

In our case, because X is the end-to-end SIR and $F_X(x)$ is the outage probability, it is obvious that $F_X(x) = 0$ for $x < 0$, and thus (52) can be simplified to

$$\mathbb{E}\{X\} = \int_0^{\infty} (1 - F_X(x))\mathrm{d}x. \tag{53}$$

Considering $F_X(x)$ is a monotone increasing function of x, the relation given in (53) validates the equivalence between $\min\limits_{\alpha}\{P_{out}(s)\}$ and $\max\limits_{\alpha}\{\mathbb{E}\{\Gamma_{SR_nD}(k)\}\}$, for $0 < \alpha < 1$.

Appendix B
Proof of Quasi-Concavity of the Optimization Problem Formulated in (46)

To prove the quasi-concavity of the formulated problem in (46), we first propose a lemma as follows:

Lemma 1: Given a bounded, continuous and real piecewise function

$$f(x) = \begin{cases} f_1(x), & x \in (x_{\min}, x_c) \\ f_2(x), & x \in [x_c, x_{\max}) \end{cases}, \tag{54}$$

if $f_1(x)$ is a monotone increasing function of x, and $f_2(x)$ is a monotone decreasing function of x, $f(x)$ is a quasi-concave function of x and the maximum $f(x)$ is achieved when $x = x_c$.

Proof: This lemma is straightforward to prove by elementary algebraic derivations and the definition of a quasi-concave function. Therefore, we omit a detailed proof here, and comprehensive analysis of the relation between quasi-concavity and monotonicity can be found in [41]. ∎

As a result of *Lemma 1*, we can transfer the exploration of quasi-concavity to the explorations of continuity and monotonicity. It is obvious from (47b) and (47c) that $\omega_1(\alpha)$ and $\omega_2(\alpha)$ are continuous over $\alpha \in (0, \varrho)$ and $\alpha \in [\varrho, 1)$. Now, we can examine the continuity of both $\omega_1(\alpha)$ and $\omega_2(\alpha)$ at the boundary point $\alpha = \varrho$ by

$$\lim_{\alpha \to \varrho^-} \omega_i(\alpha) = \lim_{\alpha \to \varrho^+} \omega_i(\alpha), \tag{55}$$

where $i \in \{1, 2\}$. This relation indicates that both $\omega_1(\alpha)$ and $\omega_2(\alpha)$ are continuous at the boundary point $\alpha = \varrho$. Therefore, both $\omega_1(\alpha)$ and $\omega_2(\alpha)$ are continuous over the entire domain of definition $\alpha \in (0, 1)$.

To investigate the monotonicity of $\omega_1(\alpha)$ and $\omega_2(\alpha)$, we propose another two lemmas as follows:

Lemma 2: $f(x) = Ax\left(1 - e^{-\frac{B}{x}}\right)$, where A and B are bounded and positive constants, is a monotone increasing function of x, $\forall\ x \in (0, 1)$.

Proof: We derive the first and second order derivatives of $f(x)$ with respect to x as follows:

$$f'(x) = \frac{\mathrm{d}f(x)}{\mathrm{d}x} = A\left(1 - \frac{B + x}{x} e^{-\frac{B}{x}}\right) \tag{56}$$

and

$$f''(x) = \frac{\mathrm{d}^2 f(x)}{\mathrm{d}x^2} = -\frac{AB^2}{x^3} e^{-\frac{B}{x}} < 0. \tag{57}$$

From (57), we know that $f'(x)$ is a monotone decreasing function of x and therefore

$$\min_x \{f'(x)\} > \lim_{x \to 1} f'(x) = Ae^{-B}\left(e^B - B - 1\right) > 0. \tag{58}$$

Because the first order derivative $f'(x) > 0$, $\forall\ x \in (0, 1)$, $f(x)$ is a monotone increasing function of x. ∎

Lemma 3: $t(x) = A(1 - x)\left(1 - e^{-\frac{B}{1-x}}\right)$, where A and B are bounded and positive constants, is a monotone decreasing function of x, $\forall\ x \in (0, 1)$.

Proof: We can express $t(x) = f(1-x)$. By *Lemma 2*, $f(x)$ is a monotone increasing function of x, and $f'(x) > 0$, $\forall\ x \in (0, 1)$. Then, we can obtain the first order derivative of $t(x)$ with respect to x by

$$t'(x) = \frac{\mathrm{d}t(x)}{\mathrm{d}x} = \frac{\mathrm{d}f(1-x)}{\mathrm{d}x} = -f'(x) < 0, \tag{59}$$

and therefore $t(x) = f(1 - x)$ is a monotone decreasing function of x, $\forall\ x \in (0, 1)$. ∎

According to *Lemma 2* and *Lemma 3*, we can easily see that $\omega_1(\alpha)$ and $\omega_2(\alpha)$ are monotone increasing functions of α when $0 < \alpha < \varrho$ and monotone decreasing functions of α when $\varrho \leq \alpha < 1$. As a result of *Lemma 1*, we prove that $\omega_1(\alpha)$ and $\omega_2(\alpha)$ are quasi-concave functions of x, $\forall\ x \in (0, 1)$, and so as the quasi-concavity of the formulated problem in (46).

Appendix C
Proof of Quasi-Concavity of the Optimization Problem Formulated in (48)

It can be easily seen that $\gamma_1(\alpha)$ is a bounded, continuous and monotone increasing function of α, while $\gamma_2(\alpha)$ is a bounded, continuous and monotone decreasing function of α. To prove $\gamma(\alpha)$ to be a quasi-concave function of α, we first divide the formulated problem into three cases:

1) Case 1: $\gamma_1(\alpha) > \gamma_2(\alpha)$, $\forall\ \alpha \in (0, 1)$.
2) Case 2: $\gamma_1(\alpha) < \gamma_2(\alpha)$, $\forall\ \alpha \in (0, 1)$.
3) Case 3: $\gamma_1(\alpha) < \gamma_2(\alpha)$, for $\alpha \in (0, \epsilon)$, and $\gamma_1(\alpha) > \gamma_2(\alpha)$, $\forall\ \alpha \in (\epsilon, 1)$, where ϵ is a critical point in which $\gamma_1(\epsilon) = \gamma_2(\epsilon)$.

For Case 1 and Case 2, it is straightforward that $\gamma(\alpha) = \gamma_1(\alpha)$ and $\gamma(\alpha) = \gamma_2(\alpha)$. Because of the monotonicity of $\gamma_1(\alpha)$ and $\gamma_2(\alpha)$, it is easy to derive the relation infra for both cases

$$\begin{aligned} &\forall\ \alpha_1, \alpha_2 \in (0, 1) \text{ and } \lambda \in (0, 1), \\ &\quad \exists\ \gamma(\lambda\alpha_1 + (1 - \lambda)\gamma_2) \geq \min\left\{\gamma(\alpha_1), \gamma(\gamma_2)\right\}. \end{aligned} \tag{60}$$

Hence, according to the definition of a quasi-concave function [42], we have proved $\gamma(\alpha)$ to be quasi-concave for Case 1 and Case 2. For Case 3, we suppose $0 < \alpha_1 < \alpha_2 < 1$ without losing generality and further divide Case 3 into another three sub-cases as follows:

1) Case 3-1: $0 < \alpha_1 < \alpha_2 < \epsilon$
2) Case 3-2: $\epsilon < \alpha_1 < \alpha_2 < 1$
3) Case 3-3: $0 < \alpha_1 < \epsilon < \alpha_2 < 1$

Case 3-1 and Case 3-2 are simply special cases of Case 2 and Case 1, respectively. Therefore, the quasi-concavity of Case 3-1 and Case 3-2 can be proved in a similar manner as above. For Case 3-3, we need to discuss λ in the range of $\left(0, \frac{\alpha_2 - \epsilon}{\alpha_2 - \alpha_1}\right)$ and $\left(\frac{\alpha_2 - \epsilon}{\alpha_2 - \alpha_1}, 1\right)$, respectively. When $\lambda \in \left(0, \frac{\alpha_2 - \epsilon}{\alpha_2 - \alpha_1}\right)$, we can derive

$$\begin{aligned} \gamma(\lambda\alpha_1 + (1 - \lambda)\alpha_2) &= \gamma_1(\lambda\alpha_1 + (1 - \lambda)\alpha_2) \\ &\geq \gamma_1(\alpha_1) = \gamma(\alpha_1) \geq \min\{\gamma(\alpha_1), \gamma(\alpha_2)\}. \end{aligned} \tag{61}$$

Similarly, when $\lambda \in \left(\frac{\alpha_2 - \epsilon}{\alpha_2 - \alpha_1}, 1\right)$, we can derive

$$\begin{aligned} \gamma(\lambda\alpha_1 + (1 - \lambda)\alpha_2) &= \gamma_2(\lambda\alpha_1 + (1 - \lambda)\alpha_2) \\ &\geq \gamma_2(\alpha_2) = \gamma(\alpha_2) \geq \min\{\gamma(\alpha_1), \gamma(\alpha_2)\}. \end{aligned} \tag{62}$$

By (61) and (62), we have proved $\gamma(\alpha)$ to be a quasi-concave function of α for Case 3. Now, we have proved $\gamma(\alpha)$ to be a quasi-concave function of α for all cases and thus the quasi-concavity of the formulated optimization problem.

Acknowledgment

The authors would like to thank the editor and the anonymous reviewers for their constructive comments which help improve the quality of this paper.

References

[1] M. N. Tehrani, M. Uysal, and H. Yanikomeroglu, "Device-to-device communication in 5G cellular networks: challenges, solutions, and future directions," *IEEE Communications Magazine*, vol. 52, no. 5, pp. 86–92, May 2014.

[2] A. Asadi, Q. Wang, and V. Mancuso, "A survey on device-to-device communication in cellular networks," *IEEE Commun. Surveys Tutorials*, vol. 16, no. 4, pp. 1801–1819, 2014.

[3] M. Sheng, Y. Li, X. Wang, J. Li, and Y. Shi, "Energy efficiency and delay tradeoff in device-to-device communications underlaying cellular networks," *IEEE J. Sel. Areas in Commun.*, vol. 34, no. 1, pp. 92–106, Jan. 2016.

[4] H. A. U. Mustafa, M. A. Imran, M. Z. Shakir, A. Imran, and R. Tafazolli, "Separation framework: an enabler for cooperative and D2D communication for future 5G networks," *IEEE Communications Surveys Tutorials*, vol. 18, no. 1, pp. 419–445, 2016.

[5] X. Lin, J. G. Andrews, and A. Ghosh, "Spectrum sharing for device-to-device communication in cellular networks," *IEEE Transactions on Wireless Communications*, vol. 13, no. 12, pp. 6727–6740, Dec. 2014.

[6] Z. Zhang, Z. Ma, M. Xiao, Z. Ding, and P. Fan, "Full-duplex device-to-device-aided cooperative nonorthogonal multiple access," *IEEE Transactions on Vehicular Technology*, vol. 66, no. 5, pp. 4467–4471, May 2017.

[7] J. Zhao, Y. Liu, K. K. Chai, Y. Chen, M. Elkashlan, and J. Alonso-Zarate, "NOMA-based D2D communications: towards 5G," in *Proc. IEEE GLOBECOM*, Washington, DC, USA, Dec. 2016.

[8] Y. Ni, X. Wang, S. Jin, K. K. Wong, H. Zhu, and N. Zhang, "Outage probability of device-to-device communication assisted by one-way amplify-and-forward relaying," *IET Communications*, vol. 9, no. 2, pp. 271–282, 2015.

[9] X. Ma, R. Yin, G. Yu, and Z. Zhang, "A distributed relay selection method for relay assisted device-to-device communication system," in *Proc. IEEE PIMRC*, Sydney, NSW, Australia, Sept. 2012.

[10] J. F. Shi, L. Tao, M. Chen, and Z. H. Yang, "Power control for relay-assisted device-to-device communication underlaying cellular networks," in *Proc. IEEE WCSP*, Nanjing, China, Oct. 2015.

[11] A. Al-Hourani, S. Kandeepan, and E. Hossain, "Relay-assisted device-to-device communication: a stochastic analysis of energy saving," *IEEE Transactions on Mobile Computing*, vol. 15, no. 12, pp. 3129–3141, Dec. 2016.

[12] Y. Yang, Y. Zhang, L. Dai, J. Li, S. Mumtaz, and J. Rodriguez, "Transmission capacity analysis of relay-assisted device-to-device overlay/underlay communication," *IEEE Transactions on Industrial Informatics*, vol. 13, no. 1, pp. 380–389, Feb. 2017.

[13] R. Ma, Y. J. Chang, H. H. Chen, and C. Y. Chiu, "On relay selection schemes for relay-assisted D2D communications in LTE-A systems," *IEEE Transactions on Vehicular Technology*, 2017.

[14] G. Zhang, K. Yang, P. Liu, and J. Wei, "Power allocation for full-duplex relaying-based D2D communication underlaying cellular networks," *IEEE Transactions on Vehicular Technology*, vol. 64, no. 10, pp. 4911–4916, Oct. 2015.

[15] B. Zhong, J. Zhang, Q. Zeng, and X. Dai, "Coverage probability analysis for full-duplex relay aided device-to-device communications networks," *China Communications*, vol. 13, no. 11, pp. 60–67, Nov. 2016.

[16] S. Dang, G. Chen, and J. P. Coon, "Outage performance analysis of full-duplex relay-assisted device-to-device systems in uplink cellular networks," *IEEE Transactions on Vehicular Technology*, vol. 66, no. 5, pp. 4506–4510, May 2017.

[17] J. G. Andrews, S. Buzzi, W. Choi, S. V. Hanly, A. Lozano, A. C. K. Soong, and J. C. Zhang, "What will 5G be?" *IEEE Journal on Selected Areas in Communications*, vol. 32, no. 6, pp. 1065–1082, Jun. 2014.

[18] P. Wu, P. C. Cosman, and L. B. Milstein, "Resource allocation for multicarrier device-to-device video transmission: symbol error rate analysis and algorithm design," *IEEE Transactions on Communications*, 2017.

[19] S. Dang, J. P. Coon, and G. Chen, "Resource allocation for full-duplex relay-assisted device-to-device multicarrier systems," *IEEE Wireless Communications Letters*, vol. 6, no. 2, pp. 166–169, Apr. 2017.

[20] C. Y. Wong, R. S. Cheng, K. B. Lataief, and R. D. Murch, "Multiuser OFDM with adaptive subcarrier, bit, and power allocation," *IEEE Journal on Selected Areas in Communications*, vol. 17, no. 10, pp. 1747–1758, Oct. 1999.

[21] S. Yin and Z. Qu, "Resource allocation in multiuser OFDM systems with wireless information and power transfer," *IEEE Communications Letters*, vol. 20, no. 3, pp. 594–597, Mar. 2016.

[22] G. Chen, D. Liang, M. Ghoraishi, P. Xiao, and R. Tafazolli, "Optimum user selection for hybrid-duplex device-to-device in cellular networks," in *Proc. IEEE ISWCS*, Brussels, Belgium, Aug. 2015.

[23] B. Kaufman and B. Aazhang, "Cellular networks with an overlaid device-to-device network," in *Proc. IEEE ACSSC*, Pacific Grove, CA, Oct. 2008.

[24] G. Chen, Y. Gong, P. Xiao, and J. A. Chambers, "Dual antenna selection in secure cognitive radio networks," *IEEE Transactions on Vehicular Technology*, vol. 65, no. 10, pp. 7993–8002, Oct. 2016.

[25] I. Krikidis, "Relay selection for two-way relay channels with MABC DF: a diversity perspective," *IEEE Transactions on Vehicular Technology*, vol. 59, no. 9, pp. 4620–4628, Nov. 2010.

[26] X. Wu, Y. Shen, and Y. Tang, "Propagation characteristics of the full-duplex self-interference channel for the indoor environment at 2.6 GHz," in *Proc. IEEE APSURSI*, Jul. 2014.

[27] M. Duarte, C. Dick, and A. Sabharwal, "Experiment-driven characterization of full-duplex wireless systems," *IEEE Transactions on Wireless Communications*, vol. 11, no. 12, pp. 4296–4307, Dec. 2012.

[28] M. Hasan, E. Hossain, and D. I. Kim, "Resource allocation under channel uncertainties for relay-aided device-to-device communication underlaying LTE-A cellular networks," *IEEE Transactions on Wireless Communications*, vol. 13, no. 4, pp. 2322–2338, Apr. 2014.

[29] S. Dang, J. P. Coon, and G. Chen, "An equivalence principle for OFDM-based combined bulk/per-subcarrier relay selection over equally spatially correlated channels," *IEEE Transactions on Vehicular Technology*, vol. 66, no. 1, pp. 122–133, Jan. 2017.

[30] Y. Li, W. Wang, and F. C. Zheng, "Combined bulk and per-tone relay selection in cooperative OFDM systems," in *Proc. IEEE ICCC*, Beijing, China, Aug. 2012.

[31] L. Dai, B. Gui, and L. J. C. Jr., "Selective relaying in OFDM multihop cooperative networks," in *Proc. IEEE WCNC*, Kowloon, Hong Kong, China, Mar. 2007.

[32] W. Yang and Y. Cai, "On the performance of the block-based selective OFDM decode-and-forward relaying scheme for 4G mobile communication systems," *Journal of Communications and Networks*, vol. 13, no. 1, pp. 56–62, Feb. 2011.

[33] Z. Zhang, K. Long, A. V. Vasilakos, and L. Hanzo, "Full-duplex wireless communications: challenges, solutions, and future research directions," *Proceedings of the IEEE*, vol. 104, no. 7, pp. 1369–1409, Jul. 2016.

[34] R. Merris, *Combinatorics*, ser. Wiley Series in Discrete Mathematics and Optimization. Wiley, 2003.

[35] F.-C. Chang, "Recursive formulas for the partial fraction expansion of a rational function with multiple poles," *Proceedings of the IEEE*, vol. 61, no. 8, pp. 1139–1140, Aug. 1973.

[36] H. Kung and D. Tong, "Fast algorithms for partial fraction decomposition," *SIAM Journal on Computing*, vol. 6, no. 3, pp. 582–593, 1977.

[37] P. Sun, K. G. Shin, H. Zhang, and L. He, "Transmit power control for D2D-underlaid cellular networks based on statistical features," *IEEE Transactions on Vehicular Technology*, vol. 66, no. 5, pp. 4110–4119, May 2017.

[38] M. Grant, S. Boyd, and Y. Ye, "CVX: Matlab software for disciplined convex programming," 2008.

[39] T. K. Baranwal, D. S. Michalopoulos, and R. Schober, "Outage analysis of multihop full duplex relaying," *IEEE Communications Letters*, vol. 17, no. 1, pp. 63–66, Jan. 2013.

[40] B. Hajek, "Notes for ECE 534 an exploration of random processes for engineers," *Univ. of Illinois at Urbana–Champaign*, 2009.

[41] A. Guerraggio and E. Molho, "The origins of quasi-concavity: a development between mathematics and economics," *Historia Mathematica*, vol. 31, no. 1, pp. 62–75, 2004.

[42] A. C. E. Kenneth J. Arrow, "Quasi-concave programming," *Econometrica*, vol. 29, no. 4, pp. 779–800, 1961.

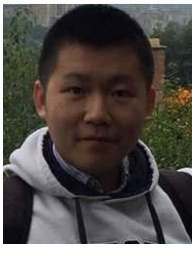

Shuping Dang (S'13) received the B.Eng (Hons) degree in Electrical and Electronic Engineering from the University of Manchester (with first class honors) and the B.Eng in Electrical Engineering and Automation from Beijing Jiaotong University in 2014 via a joint '2+2' dual-degree program. He was also a *Certified LabVIEW Associate Developer* (CLAD) by National Instrument (NI) (2014 - 2016). Mr. Dang is currently a D.Phil candidate with the Department of Engineering Science, University of Oxford and serves as a reviewer for IEEE TRANSACTIONS ON WIRELESS COMMUNICATIONS, IEEE TRANSACTIONS ON COMMUNICATIONS, IEEE TRANSACTIONS ON VEHICULAR TECHNOLOGY, DIGITAL SIGNAL PROCESSING, EURASIP JOURNAL ON WIRELESS COMMUNICATIONS AND NETWORKING as well as the TPC member of a number of leading conferences in communication engineering. His current research interests include cooperative communications, multi-carrier systems, device-to-device communications and index modulation.

Gaojie Chen (S'09-M'12) received the B.Eng. and B.Ec. degrees in electrical information engineering and international economics and trade from Northwest University, China, in 2006, and the M.Sc. (Hons.) and Ph.D. degrees in electrical and electronic engineering from Loughborough University, Loughborough, U.K., in 2008 and 2012, respectively. From 2008 to 2009, he was a Software Engineering with DTmobile, Beijing, China, and from 2012 to 2013, he was a Research Associate with the School of Electronic, Electrical and Systems Engineering, Loughborough University. He was a Research Fellow with 5GIC, Faculty of Engineering and Physical Sciences, University of Surrey, U.K., from 2014 to 2015. Then he was a Research Associate with the Department of Engineering Science, University of Oxford, U.K., from 2015 to 2018. He is currently a Lecturer with the Department of Engineering, University of Leicester, U.K. He has served as an Editor for IET ELECTRONICS LETTERS (2018-present). His current research interests include information theory, wireless communications, cooperative communications, cognitive radio, secrecy communication, and random geometric networks.

Justin P. Coon (S'02-M'05-SM'10) received a BSc. degree (with distinction) in electrical engineering from the Calhoun Honours College, Clemson University, USA and a Ph.D in communications from the University of Bristol, U.K. in 2000 and 2005, respectively. In 2004, he joined Toshiba Research Europe Ltd. (TREL) as a Research Engineer working in its Bristol based Telecommunications Research Laboratory (TRL), where he conducted research on a broad range of communication technologies and theories, including single and multi-carrier modulation techniques, estimation and detection, diversity methods, system performance analysis and networks. He held the position of Research Manager from 2010-2013, during which time he led all theoretical and applied research on the physical layer at TRL. Dr Coon was a Visiting Fellow with the School of Mathematics at the University of Bristol from 2010-2012, and held a position as Reader in the Department of Electrical and Electronic Engineering at the same university from 2012-2013. He joined the University of Oxford in 2013 where he is currently an Associate Professor with the Department of Engineering Science and a Tutorial Fellow of Oriel College.

Dr Coon is the recipient of TRLs Distinguished Research Award for his work on block-spread CDMA, aspects of which have been adopted as mandatory features in the 3GPP LTE Rel-8 standard. He is also a co-recipient of two 'best paper' awards for work presented at ISWCS 13 and EuCNC 14. Dr Coon has published in excess of 150 papers in leading international journals and conferences, and is a named inventor on more than 30 patents. He served as an Editor for IEEE TRANSACTIONS ON WIRELESS COMMUNICATIONS (2007 - 2013), IEEE TRANSACTIONS ON VEHICULAR TECHNOLOGY (2013 - 2016), IEEE WIRELESS COMMUNICATIONS LETTERS (2016 - present) and IEEE COMMUNICATIONS LETTERS (2017 - present). Dr Coon's research interests include communication theory, information theory and network theory.